AIMS Materials Science, 8(5): 836–851.
DOI: 10.3934/matersci.2021051
Received: 28 June 2021
Accepted: 31 October 2021
Published: 30 November 2021

http://www.aimspress.com/journal/Materials

Research article

Influence of normalizing post carburizing treatment on microstructure, mechanical properties and fracture behavior of low alloy gear steels

Pavan Hiremath, Gowrishankar M. C., Manjunath Shettar, Sathyashankara Sharma*, Jayashree P. K. and Suhas Kowshik

Department of Mechanical and Manufacturing Engineering, Manipal Institute of Technology, Manipal Academy of Higher Education, Manipal, Karnataka, India

* **Correspondence:** Email: ss.sharma@manipal.edu; Tel: +919740540928; Fax: +918202571071.

Abstract: Steel is a versatile metal, got a wide range of applications in all the fields of engineering and technology. Generally, low carbon steels are tough and high alloy carbon steels are hard in nature. Certain applications demand both properties in the same steel. Carburization is one such technique that develops hard and wear resistant surfaces with a soft core. The objective of this work is to study the influence of post carburizing treatment (normalizing) on three grades of steels (EN 3, 20MnCr5, and EN 353). Post carburizing treatments are necessary to overcome the adverse effects of carburization alone. Here carburization was carried out in the propane atmosphere by heating the gas carburizing furnace to 930 ºC for more than a day. Normalizing was carried out at 870 ºC for 1 h and cooled in air. Tensile, hardness, Charpy impact tests along with SEM (scanning electron microscopy) and EDAX (energy dispersive X-ray analysis) were conducted to analyze the phase transformation, failure mode analysis in all the samples. Carburized steels displayed the formation of ferrite, pearlite, and sometimes bainite phases in the core and complete coarse pearlite in the case regions, whereas in the post carburized steels, increased amount of ferrite, fine pearlite, and bainite in the core and fine pearlite with traces of bainite in the case region was observed. Normalizing also refines the grain with increased UTS (ultimate tensile strength), hardness, and impact resistance. EN 353 showed higher UTS among the steels with 898 MPa after carburization and 1370 MPa after normalizing treatment. Maximum hardness of 48 HRC was observed in 20MnCr5 and toughness was superior in EN 3 with energy absorbed during test i.e., 8 and 12 J before and after normalizing treatment. Based on the fracture surface analysis, in EN 353 steel, a finer array of dimples with voids and elongated bigger clustered dimples containing ultrafine dimples array are observed in the core and case respectively during carburizing whereas, more density of river pattern and cleavage failure (brittle) are observed in the core and case respectively after post carburizing (normalizing) treatment. There is

a reduction in the ductility of the steels after post carburizing treatment. It was observed that normalizing treatment produces superior mechanical properties in the carburized steels by grain refinement and strong microstructures like bainite. Normalizing as post carburizing treatment can be recommended for engineering applications where ductile core and hard surface are of great importance.

Keywords: carburization; normalizing treatment; pearlite; interlamellar distance; bainite

1. Introduction

Carburization is a thermo-chemical heat treatment commonly employed to enhance the surface (wear) as well as bulk mechanical properties of low carbon steels. This is one of the most effective and widely used methods of case hardening treatments in industries. Carburization produces harder and wear resistant surfaces along with tougher and impact resistant cores [1–3]. Sometimes carburization alone may not give out the required properties, which necessitates certain heat treatments after carburization called post carburizing treatments to reach the required quality [4,5]. Components of automobiles such as gears, cams, shafts, etc., which require shock resisting properties along with wear resistant surfaces are usually carburized. Normally, the steels containing a carbon content of around 0.2 wt% or less are considered as carburizing grade steels. During carburization, the carbon concentration in the steel's surface is enriched up to 0.9 wt%, whereas the inner core remains unchanged [6–8].

The practice of carburization is employed on the steels for the past several hundred years. In recent days it is been carried out in sophisticated ways. In this study, the steel specimens are heated to austenitizing temperature and gas carburized in a carbon rich environment. After carburization, the samples were cooled in the same furnace. As the steels are slowly cooled from the austenitizing temperature, the resultant structure contains a coarse colony of pearlite and ferrite [9]. The higher carbon content in the surface and the coarser grains in the steel result in higher brittleness and reduced strength. Therefore, in most cases, to overcome above mentioned drawbacks, steels require specific treatments after carburization [10]. The outcome of this post carburizing heat treatment will refine the coarser grains, improve hardness at the surface and toughness in the core, relieve the continuous network of cementite along the grain boundary, and reduces the retained austenite amount [11,12]. The subsequent heat treatments followed on the carburized steel considered in this study is normalizing heat treatment as the post carburizing treatment. Most automotive and aerospace sectors are following the carburization process to improve the surface characteristics of components such as gears, shafts, cams, pistons, etc.

Normalizing treatment is carried out by heating the steel nearly 50 ºC above the upper critical temperature and holding it for a certain time where the steel completely forms the austenite phase. The temperature for normalizing varies with the carbon content in the steel [13]. The purpose of this treatment is to eliminate coarser grains, overheated structures, and elimination of carbide network by post heat treatment process to achieve required microstructure and homogenize hardness in the surface layers and enhance tensile properties and impact strength. A higher rate of cooling develops more nucleation sites which in turn reduces grain size. The resultant structure is fine pearlite with better dispersion of ferrite and cementite. This dispersion results in enhanced mechanical properties.

The grain size of normalized steel is overseen by the thickness of a part. As the cooling rate differs remarkably from case to core, there is a variation in the grain size of the normalized steel. By normalizing an optimum combination of strength and softness can be achieved [14,15].

Gramlich et al. [16] and Faccoli et al. [17] describes, normalizing heat treatment not only refines the grain size but also helps certain alloy steels to attain high strength and hard martensite structure even under air cooled condition which reduces the adverse effects of water or salt bath quenching such as quench cracks, excess brittleness, deformation, etc. According to Medynski and Janus [18], normalizing produces uniform grain size and it can also be used for cast iron to improve wear resistance, hardness, and uniformity. Based on the study made by Zheng et al. [19] and Sajid et al. [20], normalizing can reduce internal stresses in the welded and forged components. According to An et al. [21], the normalizing treatment enhances stability in the steel components by imparting "thermal memory" for successive lower temperature processes. Pandey et al. [22] justify that, the components produced by normalizing treatment will have great dimensional stability and the warpage will be under better control. Based on these superior factors, the combination of carburization and normalizing treatments may impart superlative properties in the steel components.

Since normalizing is not equilibrium cooling process we cannot predict the constituents directly referring the Fe–Carbon equilibrium diagram. Hence, the paper discusses the formation of other structures like acicular bainite, feathery bainite (non-equilibrium phases), orientation in pearlite, influence of austenite and ferrite stabilizers etc., even in air cooled (normalized) condition. Quenching is one approach whereas normalizing is another approach for property improvement. Instead of getting brittle phases by hardening followed by tempering to overcome this deficiency after carburizing, single step normalizing may result in comparable outcomes which reduces energy and time consumption. Direct quenching for the steels with alloying elements results in generation of micro cracks in the surface. For the steels with higher case depth, quenching may yield better results but there will be drastic reduction in the toughness and chips off the sharp edges when the steels are dropped, or impact loaded. This study compares the influence of different alloying elements on the microstructural and mechanical properties of three different steels.

2. Materials and methods

The chemical compositions of the steels which are considered in this study are shown in Table 1. EN 3 is unalloyed steel with a carbon content of less than 0.25 wt%. It is a common grade of steel without any alloying elements above the permissible limit, generally found in the application where heavy stress, torque, and heat treatment are not involved. 20MnCr5 has a high amount of chromium, which is a ferrite stabilizer and helps to retain ferrite even at higher temperatures thereby increasing the strength, hardness, and wear resistant properties of the steel. EN 353 has both ferrite (Cr) and austenite stabilizers (Ni) which helps in maintaining a good balance between strength and toughness.

Table 1. Composition of the test specimens.

Elements	Composition of steels (wt%)		
	EN 3	20MnCr5	EN 353
Carbon (C)	0.178	0.187	0.161
Silicon (Si)	0.188	0.203	0.255
Manganese (Mn)	0.61	1.17	0.63
Phosphorus (P)	0.017	0.0059	0.012
Sulphur (S)	0.0031	0.011	0.0080
Chromium (Cr)	-	1.11	0.84
Nickel (Ni)	-	-	1.20
Iron (Fe)	98.9	97.2	96.6

Figure 1 shows the flow chart of the methodology followed in this study. Test specimens were fabricated for tensile, impact, and hardness tests according to ASTM E8, E23, and E18 standards respectively (5 trails for each test). For microstructure analysis, specimens of diameter 20 mm were considered. The surface and subsurface region (up to 2 mm depth from surface) of the steel sample is referred as "case" and the left-out region till to the axis of specimen is referred as "core". Gas carburizing was done on the test specimens to get uniform surface carbon diffusion. Initially, degreasing of samples is done by treating in an alkaline atmosphere. All the samples were tied using metal wires and loaded into the fixtures before sending them to carburizing furnace, this helps in uniform heating and carburization of all samples. The furnace is prepared by furnace purging, where it is heated to 930 ºC with reduced intake of air for about 30 min with continuous propane addition through the spray at a rate of 1.5 L/h. This maintains positive pressure and prevents infiltration of atmospheric gas into the furnace. Purging also prevents the oxidation of steels. Once the stable atmosphere is achieved, samples were loaded into the furnace and the furnace is closed. Now propane is added to the furnace continuously through spray when the furnace heats up above 750 ºC, carburization takes place in three stages, namely: Boosting, Diffusion, and Equalizing. In boosting, samples are heated at 930 ºC for 12 hours, and the carbon potential is maintained at 0.9 to 1.1 wt% to increase diffusion rate. Boosting is followed by diffusion, here again, the samples are maintained at 930 ºC for 12 hours and carbon potential is maintained at 0.8 to 0.9 wt%. Equalizing is done by dropping the temperature to 820 ºC to avoid air hardening, here the carbon potential is maintained around 0.6 to 0.7 wt% for 1–2 hours. Finally, all the samples were cooled to room temperature in the furnace. Unburnt gases are burnt through vent holes to avoid hazardous gases entry into the atmosphere. After carburization, the carbon quantity in steel increased up to 0.764, 0.822, and 0.792 wt% in EN 3, 20MnCr5, and EN 353 respectively. For post carburizing heat treatment, the specimens were normalized by heating to 870 ºC and holding for 1 h followed by cooling in still air. As the carbon content in the surface is around eutectoid composition (0.8 wt%) and to avoid the adverse effect of higher temperatures on the steels, 870 ºC was selected for normalizing treatment. The normalized steels were tested for tensile strength using Instron 5982 UTM with 100 kN capacity. Zeiss EVO 18 special edition model was used for SEM analysis.

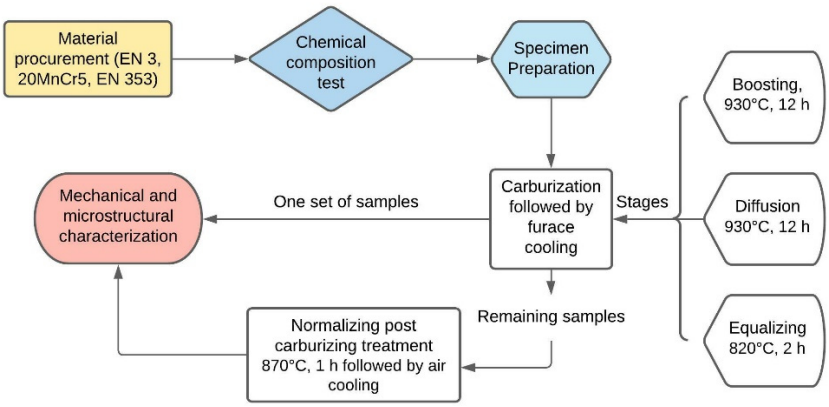

Figure 1. Flow chart of the methodology.

3. Results and discussion

Figure 2 shows the stress strain curves of selected steel grades before and after post carburization. Figure 3a,b show the microstructures of EN 3 steel at core and case respectively in carburized condition and Figure 3c,d are the microstructures of core and case respectively in post carburized (normalizing heat treatment) condition. It is observed from all the steels that there are no proeutectoid ferrite grains in the case region of the steels, indicating the effectiveness of carburization by attaining nearly eutectoid composition (It looks like, the amount of ferrite phase in post carburized core was much larger than that in the carburized core because it is representing a tiny spot where the ferrite and bainite colonies cover the entire region. Actually, ferrite colony may be still wider than shown, extension of ferrite region may not be possible to show, as higher magnification is considered). Figure 2a shows the stress strain curves for the selected three steels in carburized condition. EN 3 is plain carbon steel without any major alloying elements except carbon. In carburized condition, EN 3 displayed a definite yield point at around 295 MPa and has got highest elongation and least strength among the three grades of steel. As the steels are in furnace cooled condition and there are no major alloying elements in EN 3, developed coarser grains having grain size number around 6 in core as well as in the case. The grain size numbers of all the steels are listed in Table 2 and are measured with the help of an optical microscope and Envision software. The absence of alloying elements resulted in appreciable grain growth [23–25].

Table 2. Grain size relationships according to ASTM E 112.

Sl. no.	Type of steel	Grain size no.		Avg. grain area (μm^2)	
		Core	Case	Core	Case
1	EN 3 carburized	6	6	2016	2016
2	20MnCr5 carburized	6.5	7	1426	1008
3	EN 353 carburized	7	7	1008	1008
4	EN 3 carburized + normalized	8.5	8	356	504
5	20MnCr5 carburized + normalized	8.5	8.5	356	356
6	EN 353 carburized + normalized	9.5	9.5	178	178

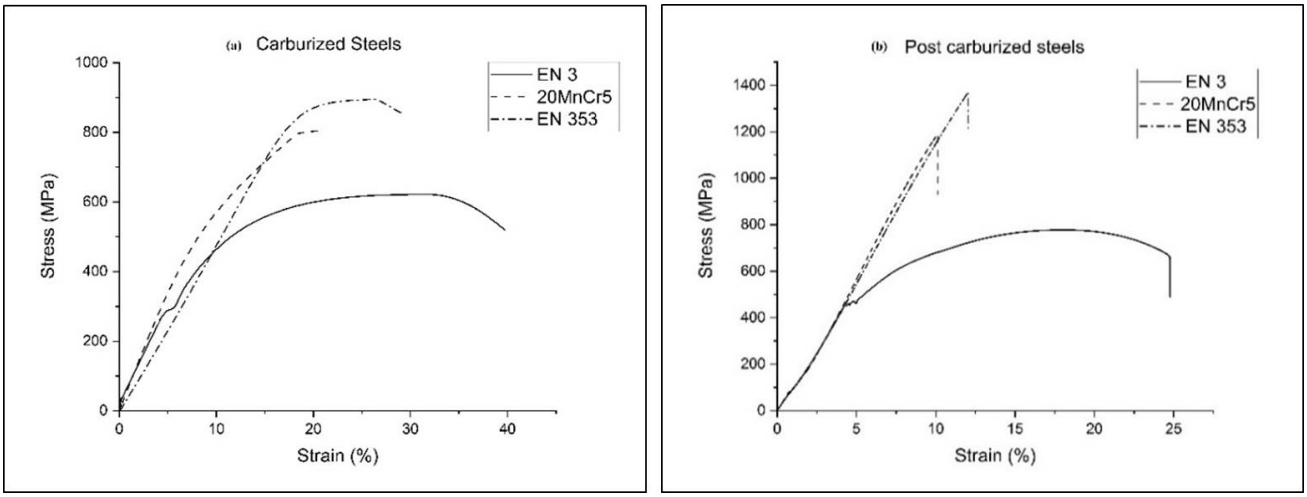

Figure 2. (a) Stress strain curves of the carburized steels and (b) stress strain curves of post carburized steels.

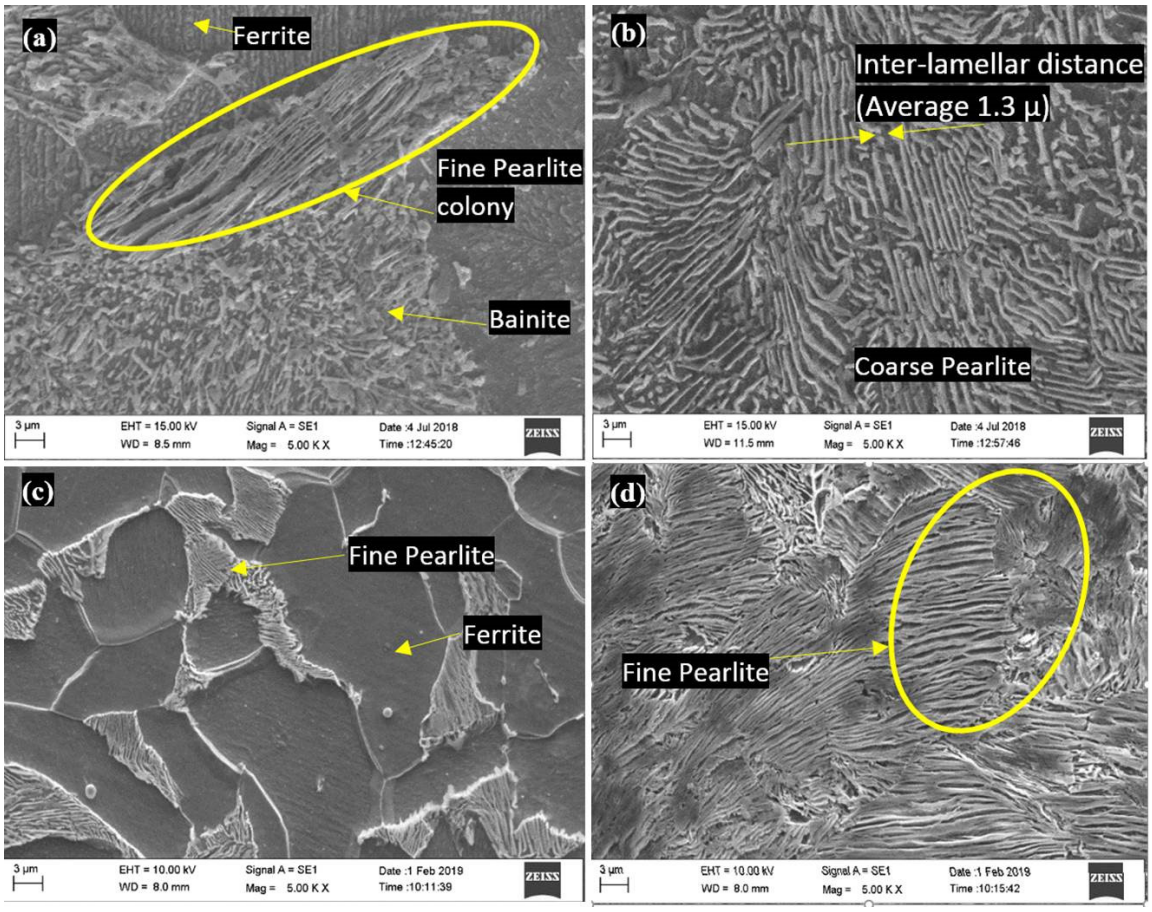

Figure 3. Microstructure of EN 3 (a) carburized core (b) carburized case (c) post carburized core (d) post carburized case.

The case region of the carburized steel developed coarse pearlite grain with an average interlamellar distance of 1.3 µm. The core region of the steel has undergone nonuniform cooling

because of different carbon concentrations and residual stress levels from the case to the core. The core microstructure shows coarser grains of ferrite and fine pearlite (0.2 μm average interlamellar spacing) along with bainitic regions as a result of a cooling curve entering both bainitic and fine pearlite regions [26,27]. Figure 3c,d show the microstructure of EN 3 after post carburizing treatment. Here, a faster rate of cooling has resulted in the formation of fine grains of pearlite and ferrite in the core, and fine grains of pearlite in the case region having grain size no. 8.5 and 8 respectively, as a result, the yield point has increased up to 470 MPa and the UTS increased to 777.7 MPa. Figure 2b shows the stress-strain curves of the steels after post carburizing treatment. Due to finer colonies of phases and an increase in area under the curve, the toughness increased after the post carburizing (normalizing) treatment.

Cr is the major alloying element in 20MnCr5 steel, and the microstructures are shown in Figure 4a,b. The core part of this steel consists of comparatively finer grains than EN 3 as shown in Table 2 and exhibited the presence of ferrite, pearlite along with feathery appearance bainite. From the microstructures, it is also clear that the bainitic region in 20MnCr5 was more than EN 3. The core region of the steel has undergone nonuniform cooling because of different carbon concentration and residual stress levels from case to the core like EN 3. The presence of Cr has affected grain growth in this steel and the cooling rate resulted in a fine structure consisting of a mixture of different phases. Cr in the steel has restricted the grain coarsening effect and increased tensile strength than EN 3. The reaction between C and Cr particles will result in the formation of chromium carbide precipitates during the slow cooling from the austenitic phase. The precipitated chromium carbide diminishes the newly generated grain boundaries and creates fine grains. Figure 5a shows the EDAX result of "region 1" in Figure 4d showing the presence of Cr, C, and Fe in the steel. 20MnCr5 did not display a definite yield point because of an increase in carbon content as well as chromium carbide precipitates. The elongation in this steel was found least when compared to EN 3 as well as EN 353 because of strong carbide former Cr. Figure 4c,d show the microstructures of core and case of 20MnCr5 respectively after post carburizing treatment. Here, the steel developed fine ferrite and bainite in the core and fine bainite in case regions. The presence of Cr has influenced the TTT curves of 20MnCr5 and resulted in bainite formation [28], even in air cooled condition. This development increased the strength of the 20MnCr5 to 1191.02 MPa and the stress strain curve is shown in Figure 2.

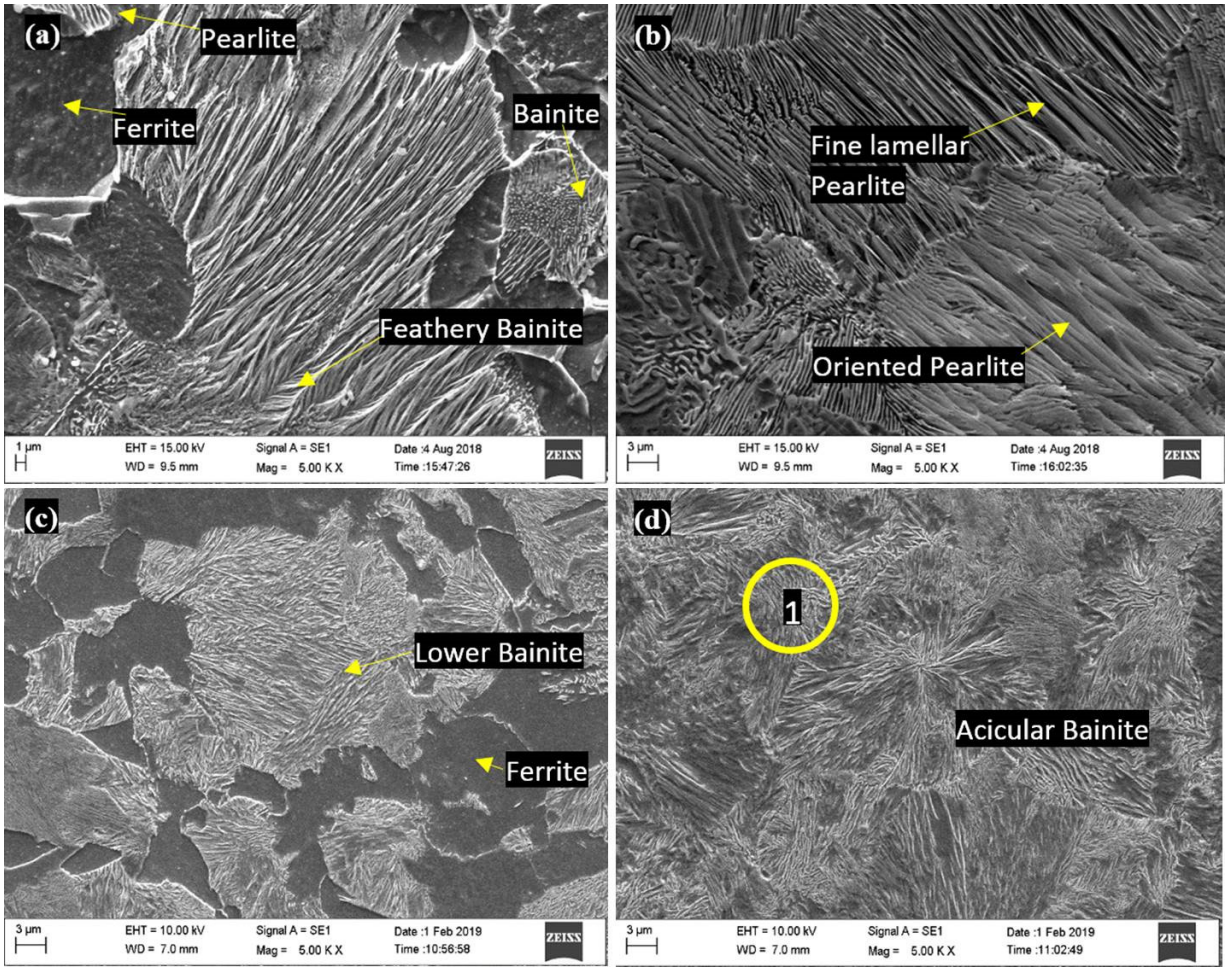

Figure 4. Microstructure of 20MnCr5 (a) carburized core (b) carburized case (c) post carburized core (d) post carburized case.

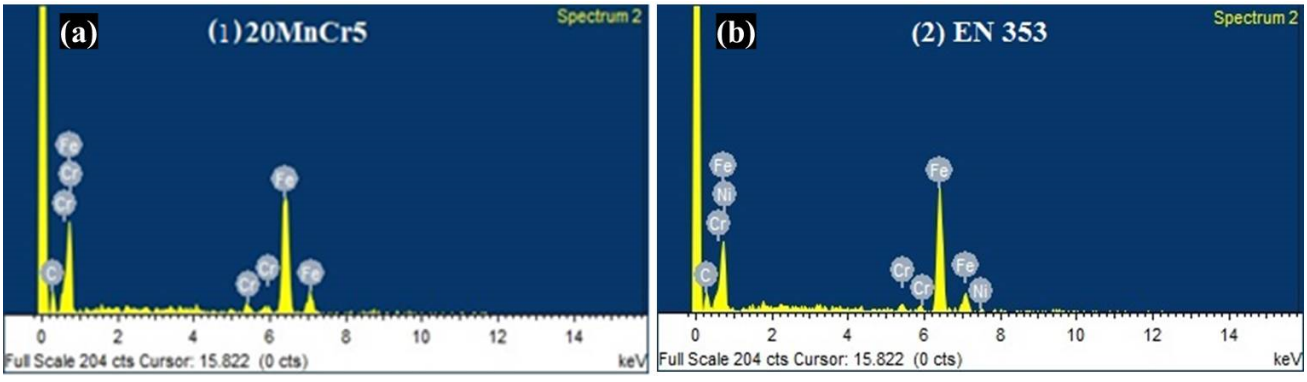

Figure 5. Energy dispersive X-ray spectroscopy results (a) 20MnCr5 (b) EN 353.

In EN 353 the major alloying elements are Cr and Ni. Cr is a strong carbide former and Ni dissolves in ferrite and increases the ductility of the steel. Figure 5b shows the EDAX result of "region 2" in Figure 6d showing the presence of Cr, Ni, C, and Fe in the steel. Microstructures of the core and case of carburized EN 353 are shown in Figure 6a,b respectively. The core region of this

steel developed fine grains of ferrite, pearlite as well as some bainite portions. The case of this steel displayed highly distorted fine-grained pearlite after carburization resulting in higher tensile strength. Ni and Cr in presence of high carbon content in the case have a greater influence on tensile strength.

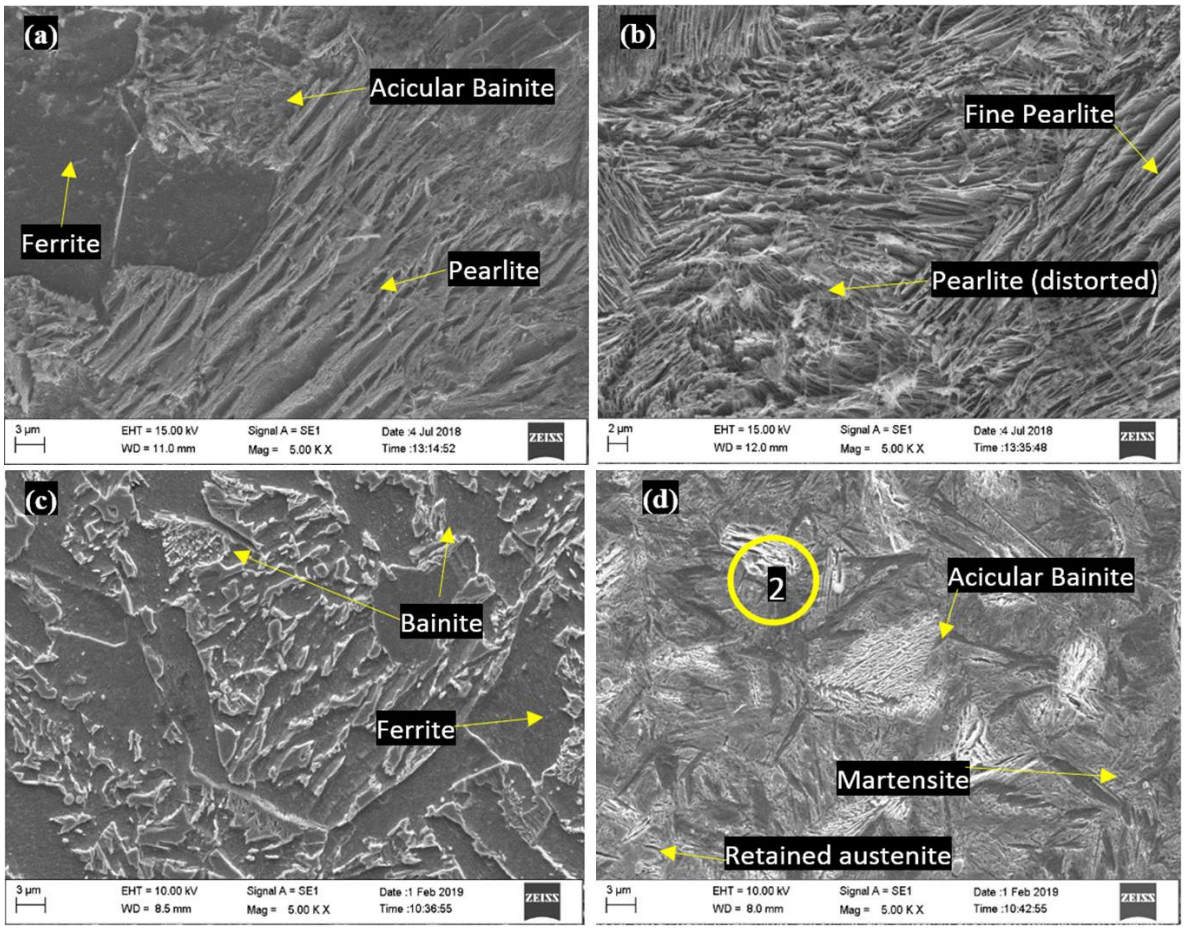

Figure 6. Microstructure of EN 353 (a) carburized core (b) carburized case (c) post carburized core (d) post carburized case.

The percentage of elongation in this steel was less when compared to EN 3 but greater when compared to 20MnCr5 because of Ni presence (austenite stabilizer). Cr alone in 20MnCr5 reduced its percentage of elongation as it forms carbides. Figure 4b shows the EDAX result of "region 2" in Figure 6d showing the presence of Cr, Ni, C, and Fe in the EN 353. Figure 6c,d show the microstructures of core and case of EN 353 respectively after post carburizing treatment. The core of this steel had formed bainite along with ferrite and the case had witnessed bainite and martensite regions along with some traces of retained austenite content, as a result, the steel received the highest strength (1370.38 MPa) after post carburizing treatment [29–31].

Figure 7 shows the tensile test results of 3 types of steels in carburized and post carburized (normalized) conditions. The UTS of post carburized steels was higher than that of carburized ones in the selected grades of steels (Figure 7a). The increment in UTS of post carburized steels was larger as the number and wt% of alloying elements in the steel increased, compared to that of respective carburized condition. This is due to the change in shape and position of the isothermal

diagram and microstructure of the steels as the alloying element increase [32,33]. Figure 7b shows the elongation (%) of tensile test specimens before fracture. The ductility (percentage of elongation) of the post carburized steel decreased in all the steel grades when compared to carburized ones due to the grain refinement as a result of a faster cooling rate. Generally, as the strength increases, the ductility of steel decreases irrespective of alloying elements [34,35]. The lowest ductility was observed in 20MnCr5, due to Cr presence, as it forms chromium carbide, which is a brittle phase.

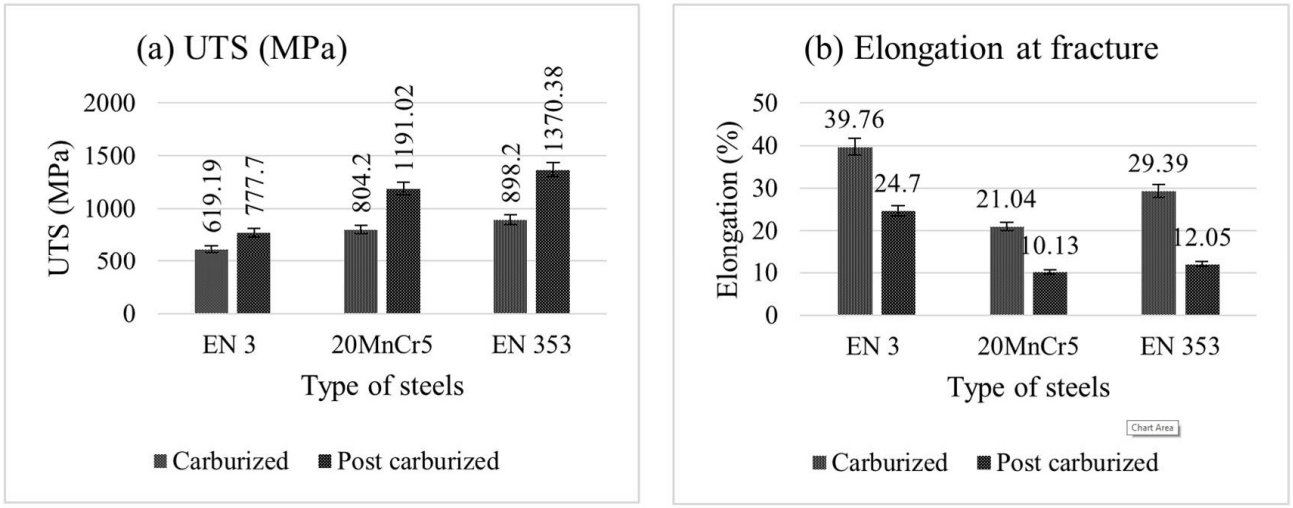

Figure 7. Results of tensile test (a) ultimate tensile strength (b) elongation at fracture.

All three grades of steels were subjected hardness test to analyze the hardness distribution. The results of this test were also in phase with the tensile test results obtained. Figure 8 shows the hardness distribution from the core to the case of the steels. As carburized steels are furnace cooled, there is a drop in the hardness of steel at the core in all the steels, but due to carburization, a large increase in the hardness in the case/surface of all steels were found. The presence of Cr in 20MnCr5 and the presence of Cr and Ni in EN 353 resulted in a higher increase of hardness in these steels. After post carburizing treatment, due to refinement of grain and change in microstructure, an increase in hardness was observed in all the steels based on their chemical composition. After normalizing treatment, the case hardness in 20MnCr was almost the same with that in EN353, however, the core hardness in 20MnCr was higher than that in EN353 due to the presence of large amount of Cr in 20MnCr5, which is a strong carbide former and has resulted in the formation of hard carbides in the steel resulting in the increased hardness in 20MnCr5 than EN 353.

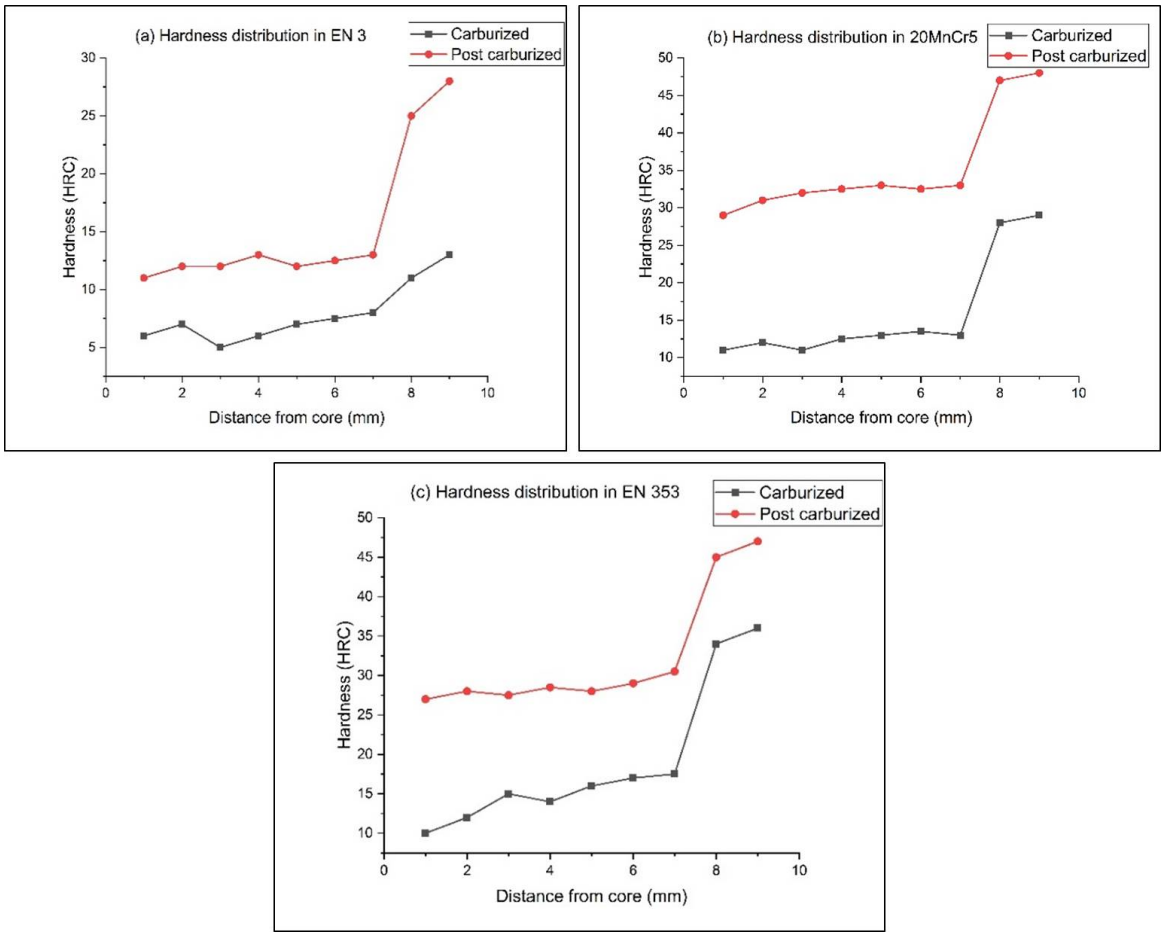

Figure 8. Hardness distribution from the core to the case of carburized and post carburized steels (a) EN 3 (b) 20MnCr5 (c) EN 353.

Figure 9 shows the energy absorbed by the steel samples during the impact test. EN 3 has got highest impact strength followed by EN 353 and 20MnCr5 displayed the least toughness. As, carbide former Cr alone in 20MnCr5 reduced its toughness, whereas in EN 353 better toughness was observed as a result of ferrite stabilizer (Cr) and austenite stabilizer (Ni). After normalizing treatment, the steels showed higher toughness because of fine grain formation. Fine grains in the microstructure deflect the crack propagation during the impact loading and increases the toughness in the steel [33].

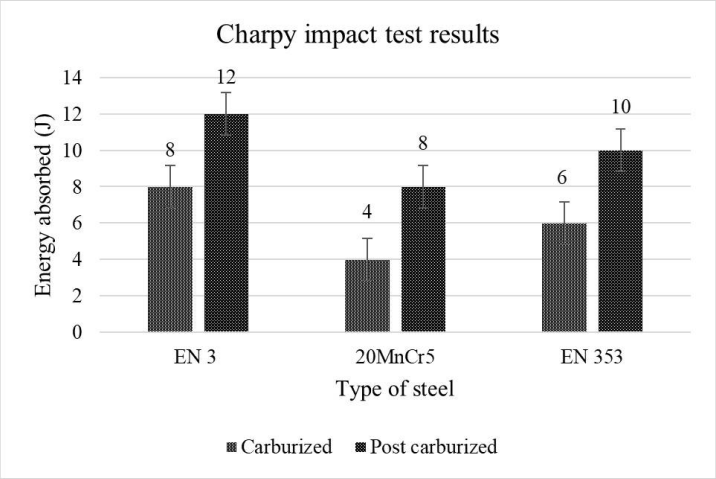

Figure 9. Energy absorbed during Charpy impact test.

Since EN 353 displayed higher hardness at the surface, good tensile properties, and reasonably good impact strength, its fracture surface was studied by SEM to analyze the fracture mode. Figure 10 shows the fracture surfaces of EN 353 before and after post carburization. EN 3, as well as 20MnCr5, displayed a similar trend during the tensile fracture. Figure 10a shows the fracture at the core of carburized steel. More number of fine equiaxial dimples on the fracture surface was observed and the fracture mode is predominantly dimple rupture. Coarser clusters containing the array of fine dimples with river patterns showing the ductile fracture of the carburized core. Figure 10c shows the fracture at the core region of post carburized steel. A considerable decrease in dimple density was observed when compared to carburized condition. In this region the fracture is due to tear and shear action, resulting in the formation of elongated dimples and river like patterns (Figure 10c). This indicates a slight reduction of ductility in the steel as a result of normalizing treatment. Figure 10b shows the fracture in the case of carburized steel. Here, no dimples were observed resulting in quasi cleavage rupture [36,37]. Quasi cleavage is localized and exhibits both dimple and cleavage fracture, but in this case, the steel exhibited predominantly cleavage or brittle fracture as a result of higher carbon content in the case. Figure 10d shows the fracture at the case of post carburized steel. At the ruptured area, a smooth and planar appearance of apparently cleavage fracture was observed. There was a very little number of shearing lines or river patterns, indicating the increase in brittleness along with certain ductility in the steel resulting in mixed mode fracture [38,39].

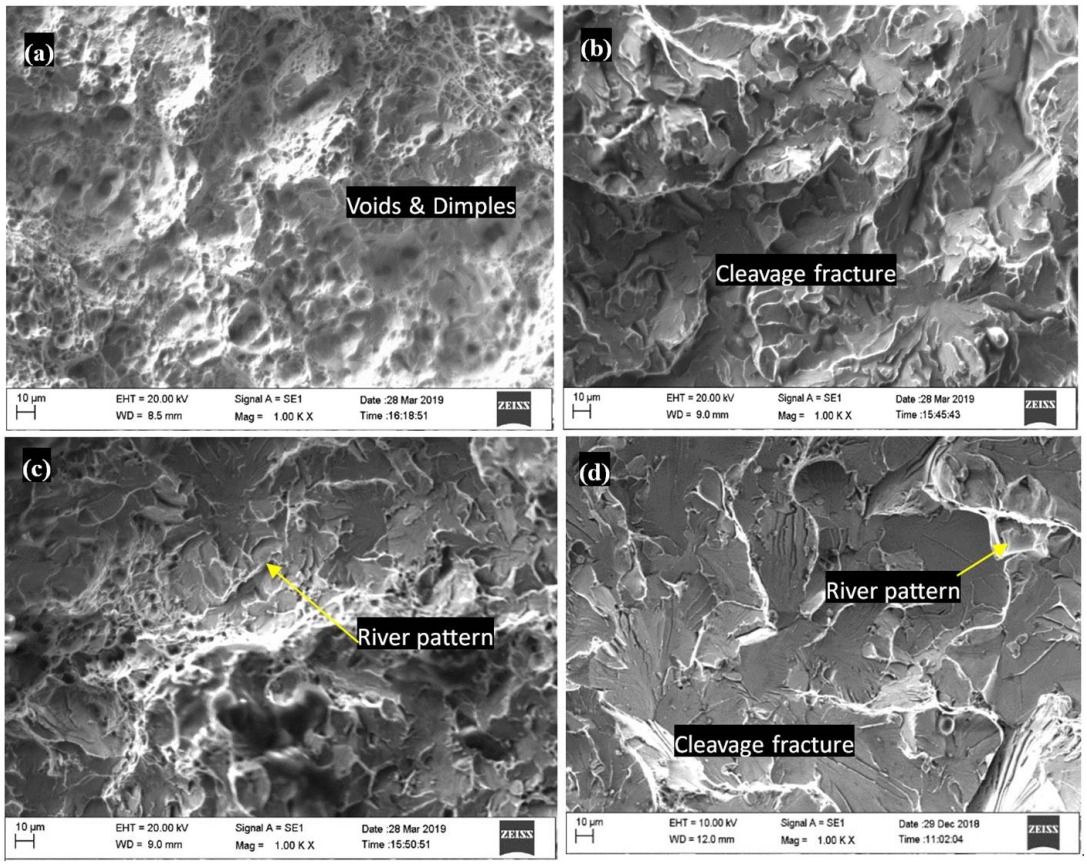

Figure 10. SEM fractographs of EN 353 (a) carburized core (b) carburized case (c) post carburized core (d) post carburized case.

4. Conclusions

The experimental work result and discussion reveal that there is provision to alter the microstructure with a change in interlamellar spacing by post carburizing treatment (normalizing). It is possible to link phase morphology and mechanical properties with fracture behavior. The three gear steels under consideration show the alloying elements responsibility (Cr and Ni) by maintaining the same level of carbon on alteration of microstructure (ferrite/bainite/martensite) concerning post carburizing treatment. No ferrite phase in the case before and after normalizing shows the attainment of eutectoid composition (0.8 wt%) after carburization. The case microstructure is pearlite before carburization and bainite after normalizing if the steel is an alloyed one. Tensile behavior (stress-strain curves), tensile, and impact strength (bar charts) show improvement in all the steels after normalizing. Grain size relationships display grain refinement after normalizing to improve hardness and its distribution, tensile and impact strengths. The study also shows EN 353 responds positively to post carburizing treatment compared to the other two steels. Fractographs of EN 353 shows fine dimples with dispersed river patterns and coarser dimples with isolated river patterns at the core before and after normalizing respectively. Similarly, both dimples with cleavage and well dispersed thin river patterns on a smooth surface at the case were observed before and after normalizing justify the results of mechanical tests conducted on the selected steels.

Conflict of interest

All authors declare no conflicts of interest in this paper.

References

1. Kajihara M (2009) Numerical analysis for migration of austenite/ferrite interface during carburization of Fe. *J Mater Sci* 44: 2109–2118.
2. Christ HJ (1998) Experimental characterization and computerbased description of the carburization behaviour of the austenitic stainless steel AISI 304L. *Mater Corros* 49: 258–265.
3. Sudha C, Bharasi NS, Anand R, et al. (2010) Carburization behavior of AISI 316LN austenitic stainless steel—Experimental studies and modeling. *J Nucl Mater* 402: 186–195.
4. Akiyama M, Oki Y, Nagai M (2012) Steam reforming of ethanol over carburized alkali-doped nickel on zirconia and various supports for hydrogen production. *Catal Today* 181:4–13.
5. Boniatti R, Bandeira AL, Crespi ÂE, et al. (2013) The influence of surface microstructure and chemical composition on corrosion behaviour in fuel-grade bio-ethanol of low-alloy steel modified by plasma nitro-carburizing and post-oxidizing. *Appl Surf Sci* 280: 156–163.
6. Yin L, Ma X, Tang G, et al. (2019) Characterization of carburized 14Cr14Co13Mo4 stainless steel by low pressure carburizing. *Surf Coat Technol* 358: 654–660.
7. Roy S, Sundararajan S (2019) Effect of retained austenite on spalling behavior of carburized AISI 8620 steel under boundary lubrication. *Int J Fatigue* 119: 238–246.
8. Lødeng R, Ranga C, Rajkhowa T, et al. (2017) Hydrodeoxygenation of phenolics in liquid phase over supported MoO_3 and carburized analogues. *Biomass Convers Biorefin* 7: 343–359.
9. Kvryan A, Efaw C, Higginbotham K, et al. (2019) Corrosion initiation and propagation on carburized martensitic stainless steel surfaces studied via advanced scanning probe microscopy. *Materials* 12: 940.
10. McLeod AC, Bishop CM, Stevens KJ, et al. (2015) Microstructure and carburization detection in HP alloy pyrolysis tubes. *Metallogr Microstruct Anal* 4: 273–285.
11. Gupta A, Singla G, Pandey OP (2016) Effect of synthesis parameters on structural and thermal properties of NbC/C nano composite synthesized via in-situ carburization reduction route at low temperature. *Ceram Int* 42: 13024–13034.
12. Niu L, Liu X, Liu X, et al. (2017) In situ XRD study on promotional effect of potassium on carburization of spray-dried precipitated Fe_2O_3 catalysts. *ChemCatChem* 9: 1691–1700.
13. Hegde A, Sharma S, Sadanand RV (2019) Mechanical characterization and optimization of heat treatment parameters of manganese alloyed austempered ductile iron. *J Mech Eng Sci* 13: 4356–4367.
14. Ahmed HM, Seetharaman S (2010) Reduction-carburization of NiO–WO_3 under isothermal conditions using H_2–CH_4 gas mixture. *Metall Mater Trans B* 41: 173–181.
15. Gutierrez-Urrutia I, Zaefferer S, Raabe D (2010) The effect of grain size and grain orientation on deformation twinning in a Fe–22wt.% Mn–0.6wt.% C TWIP steel. *Mat Sci Eng A-Struct* 527: 3552–3560.
16. Gramlich A, Schmiedl T, Schönborn S, et al. (2020) Development of air-hardening martensitic forging steels. *Mat Sci Eng A-Struct* 784: 139321.

17. Faccoli M, Ghidini A, Mazzù A (2019) Changes in the microstructure and mechanical properties of railway wheel steels as a result of the thermal load caused by shoe braking. *Metall Mater Trans A* 50: 1701–1714.
18. Medyński D, Janus A (2018) Effect of heat treatment parameters on abrasive wear and corrosion resistance of austenitic nodular cast iron Ni–Mn–Cu. *Arch Civ Mech Eng* 18: 515–521.
19. Zheng B, Shu G, Jiang Q (2019) Experimental study on residual stresses in cold rolled austenitic stainless steel hollow sections. *J Constr Steel Res* 152: 94–104.
20. Sajid HU, Kiran R (2018) Influence of stress concentration and cooling methods on post-fire mechanical behavior of ASTM A36 steels. *Constr Build Mater* 186: 920–945.
21. An JH, Lee J, Kim YS, et al. (2019) Effects of post weld heat treatment on mechanical and electrochemical properties of welded carbon steel pipe. *Met Mater Int* 25: 304–312.
22. Pandey C, Mahapatra MM, Kumar P, et al. (2018) Homogenization of P91 weldments using varying normalizing and tempering treatment. *Mat Sci Eng A-Struct* 710: 86–101.
23. Kusakin P, Belyakov A, Haase C, et al. (2014) Microstructure evolution and strengthening mechanisms of Fe–23Mn–0.3C–1.5Al TWIP steel during cold rolling. *Mat Sci Eng A-Struct* 617: 52–60.
24. Senopati G, Sutowo C, Kartika I, et al. (2019) The effect of solution treatment on microstructure and mechanical properties of Ti–6Mo–6Nb–8Sn alloy. *Mater Today Proc* 13: 224–228.
25. Bakhtiari R, Ekrami A (2009) The effect of bainite morphology on the mechanical properties of a high bainite dual phase (HBDP) steel. *Mat Sci Eng A-Struct* 525: 159–165.
26. van Bohemen SMC (2012) Bainite and martensite start temperature calculated with exponential carbon dependence. *Mater Sci Tech-Lond* 28: 487–495.
27. Yang J, Yu H, Yin J, et al. (2016) Formation and control of martensite in Ti–6Al–4V alloy produced by selective laser melting. *Mater Design* 108: 308–318.
28. Adnan F, Sajuri Z, Omar MZ (2019) Effect of uniaxial load on microstructure and mechanical properties of Thixo-joint AISI D2 tool steel. *J Mech Eng Sci* 13: 5006–5020.
29. Dmitrieva O, Ponge D, Inden G, et al. (2011) Chemical gradients across phase boundaries between martensite and austenite in steel studied by atom probe tomography and simulation. *Acta Mater* 59: 364–374.
30. Odusote K, Adekunle AS, Rabiu AB (2015) Effect of vegetable oil quenchants on the properties of aluminum during solution heat treatment. *J Mech Eng Sci* 8: 1343–1350.
31. Pandey C, Mahapatra MM, Kumar P, et al. (2017) Microstructure characterization and charpy toughness of P91 weldment for as-welded, post-weld heat treatment and normalizing & tempering heat treatment. *Met Mater Int* 23: 900–914.
32. Majid MSA, Daud R, Afendi M, et al. (2014) Stress-strain response modelling of glass fibre reinforced epoxy composite pipes under multiaxial loadings. *J Mech Eng Sci* 6: 916–928.
33. Ghadimi H, Nedjhad Sh, Eghbali B (2013) Enhanced grain refinement of cast aluminum alloy by thermal and mechanical treatment of Al–5Ti–B master alloy. *Trans Nonferrous Met Soc China* 23: 1563–1569.
34. Wang T, Cao F, Chen Z, et al. (2015) Three dimensional microstructures and wear resistance of Al–Bi immiscible alloys with different grain refiners. *Sci China Technol Sci* 58: 870–875.
35. Rosip NIM, Ahmad S, Jamaludin KR, et al. (2013) Production of 316L stainless steel (SS316L) foam via slurry method. *J Mech Eng Sci* 5: 707–712.

36. Crupi V, Epasto G, Guglielmino E, et al. (2015) Analysis of temperature and fracture surface of AISI4140 steel in very high cycle fatigue regime. *Theor Appl Fract Mec* 80: 22–30.
37. Casati R, Lemke J, Vedani M (2016) Microstructure and fracture behavior of 316L austenitic stainless steel produced by selective laser melting. *J Mater Sci Technol* 32: 738–744.
38. Rafi HK, Starr TL, Stucker BE (2013) A comparison of the tensile, fatigue, and fracture behavior of Ti–6Al–4V and 15–5 PH stainless steel parts made by selective laser melting. *Int J Adv Manuf Tech* 69: 1299–1309.
39. Pandey C, Saini N, Mahapatra MM, et al. (2017) Study of the fracture surface morphology of impact and tensile tested cast and forged (C&F) Grade 91 steel at room temperature for different heat treatment regimes. *Eng Fail Anal* 71: 131–147.

AIMS Press